Application of the Network Simulation Method To Ionic Transport in Ion-Exchange Membranes Including Diffuse Double-Layer Effects

A. A. Moya and J. Horno*

Universidad de Jaén, Departamento de Física, Facultad de Ciencias Experimentales, Paraje las Lagunillas s/n - Edificio B-3, 23071 Jaén, Spain

Received: July 30, 1999; In Final Form: October 5, 1999

The electrical properties of ion-exchange membranes have been investigated using the network simulation method. A network model is proposed for the Nernst−Planck and Poisson equations describing the ionic transport through an ion-exchange membrane and the two diffusion boundary layers on both sides of the membrane. An electric circuit simulation program is used to solve the network model in order to obtain the steady-state, transient, and small-amplitude ac electrical properties of a cation-exchange membrane in contact with an asymmetric electrolyte solution. The steady-state, chronopotentiometric, chronoamperometric, and small-amplitude ac responses of the whole membrane system have been simulated. The study is mainly intended to analyze the characteristics of the equilibrium and nonequilibrium diffuse double layers in ion-exchange membranes and to quantify some interesting aspects of the nonstationary polarization phenomena occurring at the charged membrane|solution interfaces.

1. Introduction

For a long time, the study of electrical properties of ion-exchange membranes have received considerable attention, and the literature concerning this field is extensive.[1−3] However, most of the theoretical treatments presented make use of the electroneutrality assumption in the membrane and solution phases and/or they assume the Donnan equilibrium relations at the ion-exchange membrane|solution interfaces.[4−7] Although these assumptions are approximately valid in some practical situations, they are not necessarily true when an electric current density passes through the system.[8−18] In this case, the effects of the diffuse double layers at the membrane|solution interfaces are dominant, and the problem can only be studied by examining the structure of the spatial charge regions at these interfaces.

Studies of the electrical properties of ion-exchange membranes including diffuse double-layer effects have been rare in the membrane literature,[19−21] because of the ineffectivity of the classical numerical methods to deal with situations involving the coupled, nonlinear Nernst−Planck and Poisson equations describing the ionic transport processes through ion-exchange membranes. Bassignana and Reiss[19] investigated the applicability of the assumption of local equilibrium, during steady-state transport, at only one of the interfaces between an infinitely thick ion-exchange membrane and an electrolyte solution. Selvey and Reiss[20] studied the ability of the membrane|solution interface to maintain local equilibrium, during steady-state transport, as a function of the rate of interfacial transport by using a model in which an ion-exchange membrane is in contact with an electrolyte solution. Manzanares et al.[21] numerically solved the Nernst−Planck and Poisson equations not only in the membrane|solution interfaces, as the above authors, but also in the membrane bulk and in the two diffusion boundary layers adjacent to the membrane. They analyzed, in the time domain, the complex phenomena taking place when an electric current passes through the diffuse double layers at the membrane|solution interfaces, and their results provided new physical insights into problems such as the validity of the Donnan equilibrium relations at the interfaces, the behavior of the limiting current, and the selectivity of cation-exchange membranes. However, they assumed that the diffusion coefficients of the mobile species are equal in the membrane and solution phases and do not contemplate the small-amplitude ac response in such systems. Moreover, all the previous works in this field deal only with a binary 1:1 electrolyte solution, i.e., a symmetric electrolyte. Consideration of an asymmetric electrolyte solution where the ionic diffusivities are different in the membrane and solution phases, and the simultaneous treatment of the steady-state, transient, and small-amplitude ac responses of the system complicates the problem to such an extent that it can lead to an unviable mathematical treatment.

It is here where the study of the problem by the network simulation method[22] is especially useful, since it permits serious difficulties of the mathematical analysis to be avoided. The network simulation method basically consists of modeling a physical process by means of a graphical representation analogous to circuit electrical diagrams which is analyzed by means of an electric circuit simulation program. Highly developed, commercially available software for circuit analysis can thus be employed to obtain the dynamic behavior of the whole membrane system (membrane, diffuse double layers, and diffusion boundary layers), without having to deal with the solution of the governing differential equations. The network simulation method has been previously applied to study the structure of the electrode|solution interface in electrochemical cells[22−24] and it can be satisfactorily applied to the ion-exchange membrane|solution interface.

The aim of this work is to study, using the network approach, the steady-state, transient and small-amplitude ac electrical properties of cation-exchange membranes in contact with an asymmetric electrolyte solution including diffuse double layers effects. The steady-state, chronopotentiometric, chronoamperometric, and small-amplitude ac responses of the whole mem-

* Corresponding author.

10.1021/jp992701s CCC: $18.00
Published on Web 11/19/1999

brane system have been simulated. The study is mainly intended to analyze the characteristics of the equilibrium and nonequilibrium diffuse double layers in ion-exchange membranes and to quantify some interesting aspects of the nonstationary polarization phenomena occurring at the charged membrane|solution interfaces.

2. Theory

2.1. Mathematical Model. Let us consider an ion-exchange membrane that extends from $x = 0$ to $x = d$ and two diffusion boundary layers adjacent to the membrane that extend from $x = -\delta$ to $x = 0$ and from $x = d$ to $x = d + \delta$. The membrane is bathed by two bulk solutions with the same concentration c'^0 of a 2:1 binary electrolyte. Assuming that the membrane contains fixed negatively charged groups at a uniform concentration X', and that the ionic transport is one-dimensional and perpendicular to the membrane|solution interface, in the x direction, the equations determining the behavior of the system are the continuity equations:

$$\frac{\partial J_i'(x,t)}{\partial x} = -\frac{\partial c_i'(x,t)}{\partial t}, \quad i = 1,2 \tag{1}$$

the Nernst−Planck flux equations (in dilute solution form):

$$J_i'(x,t) = -D_{ip}'\left[\frac{\partial c_i'(x,t)}{\partial x} + z_i c_i'(x,t)\frac{F}{RT}\frac{\partial \phi'(x,t)}{\partial x}\right] \tag{2}$$

and the Poisson equation:

$$\frac{\partial \mathbf{D}'(x,t)}{\partial x} = F[z_1 c_1'(x,t) + z_2 c_2'(x,t) - \theta'(x)] = \rho'(x,t) \tag{3}$$

where

$$\mathbf{D}'(x,t) = -\epsilon'\frac{\partial \phi'(x,t)}{\partial x} \tag{4}$$

and

$$\theta'(x) = \begin{cases} X', & 0 \le x \le d \\ 0, & -\delta < x < 0 \text{ and } d < x < d + \delta \end{cases} \tag{5}$$

Here $J_i'(x,t)$, D_{ip}', $c_i'(x,t)$ and z_i denote the ionic flux, the diffusion coefficient, the molar concentration, and the charge number ($z_1 = 2$ and $z_2 = -1$) of ion i, respectively. In this work, we consider the ion diffusion coefficients to be different in the diffusion boundary layers and in the ion-exchange membrane, and D_{iS}' and D_{iM}' stand for the diffusion coefficients of ion i in the solution (S) and membrane (M) phases, respectively. The electric potential is represented by $\phi'(x,t)$, the electric permittivity by ϵ', the electric displacement by $\mathbf{D}'(x,t)$, and the electric charge density by $\rho'(x,t)$. t denotes the time and the constants F, R, and T have their usual meanings.

On the other hand, the total electric current density through the membrane system, I', must be calculated in this case from the faradaic and displacement electric current densities. The total electric current density can be written as

$$I'(t) = F[z_1 J_1'(-\delta,t) + z_2 J_2'(-\delta,t)] + \frac{d\mathbf{D}'(-\delta,t)}{dt} \tag{6}$$

since it is not a function of x.[22]

It is easier to solve the Nernst−Planck and Poisson equations, using dimensionless variables. To this end, the following relations are used:

$$\xi = \frac{x}{\lambda}; \quad \tau = \frac{D_a t}{\lambda^2}$$

$$c_i = \frac{c_i'}{c_a}; \quad J_i = \frac{\lambda J_i'}{D_a c_a}; \quad D_{ip} = \frac{D_{ip}'}{D_a}; \quad i = 1,2$$

$$\phi = \frac{F\phi'}{RT}; \quad \epsilon = \frac{RT\epsilon'}{F^2 c_a \lambda^2}; \quad \mathbf{D} = \frac{\mathbf{D}'}{F c_a \lambda}; \quad \rho = \frac{\rho'}{F c_a}; \quad X = \frac{X'}{c_a}$$

$$I = \frac{\lambda I'}{F D_a c_a}$$

where D_a, c_a, and λ are scaling factors with the dimensions of diffusion coefficient, molar concentration, and length, respectively. D_a, c_a, and λ are taken as characteristic values of the system studied. In particular, we have taken $\epsilon = 1$, and so λ, given by

$$\lambda = \sqrt{\frac{\epsilon' RT}{F^2 c_a}} \tag{7}$$

can be considered as the Debye length in the system.[25] With these dimensionless parameters, eqs 1−6 can be written in the following reduced form:[22]

$$\frac{\partial J_i(\xi,\tau)}{\partial \xi} = -\frac{\partial c_i(\xi,\tau)}{\partial \tau}, \quad i = 1,2 \tag{8}$$

$$J_i(\xi,\tau) = -D_{ip}\left[\frac{\partial c_i(\xi,\tau)}{\partial \xi} + z_i c_i(\xi,\tau)\frac{\partial \phi(\xi,\tau)}{\partial \xi}\right] \tag{9}$$

$$\frac{\partial \mathbf{D}(\xi,\tau)}{\partial \xi} = z_1 c_1(\xi,\tau) + z_2 c_2(\xi,\tau) - \theta(\xi) = \rho(\xi,\tau) \tag{10}$$

$$\mathbf{D}(\xi,\tau) = -\epsilon\frac{\partial \phi(\xi,\tau)}{\partial \xi} \tag{11}$$

$$\theta(\xi) = \begin{cases} X, & 0 \le \xi \le d/\lambda \\ 0, & -\delta/\lambda < \xi < 0 \text{ and } d/\lambda < \xi < (d+\delta)/\lambda \end{cases} \tag{12}$$

$$I(\tau) = z_1 J_1\left(-\frac{\delta}{\lambda},\tau\right) + z_2 J_2\left(-\frac{\delta}{\lambda},\tau\right) + \frac{d\mathbf{D}\left(-\frac{\delta}{\lambda},\tau\right)}{d\tau} \tag{13}$$

For this system, the boundary conditions can be expressed as

$$c_1\left(-\frac{\delta}{\lambda},\tau\right) = c_1\left(\frac{d+\delta}{\lambda},\tau\right) = \frac{c^0}{2} \tag{14}$$

$$c_2\left(-\frac{\delta}{\lambda},\tau\right) = c_2\left(\frac{d+\delta}{\lambda},\tau\right) = c^0 \tag{15}$$

$$\frac{d\mathbf{D}\left(-\frac{\delta}{\lambda},\tau\right)}{d\tau} = I(\tau) - z_1 J_1\left(-\frac{\delta}{\lambda},\tau\right) - z_2 J_2\left(-\frac{\delta}{\lambda},\tau\right) \tag{16a}$$

$$\phi\left(-\frac{\delta}{\lambda},\tau\right) = \phi_A(\tau) \tag{16b}$$

$$\phi\left(\frac{d+\delta}{\lambda},\tau\right) = 0 \tag{17}$$

Equations 14−17 specify all the physical conditions to be imposed on the solution of the Nernst−Planck and Poisson equations. In particular, eqs 14 and 15 indicate that the system is electrically neutral at the outer boundaries of the diffusion boundary layers, because c_1 and c_2, respectively, have the

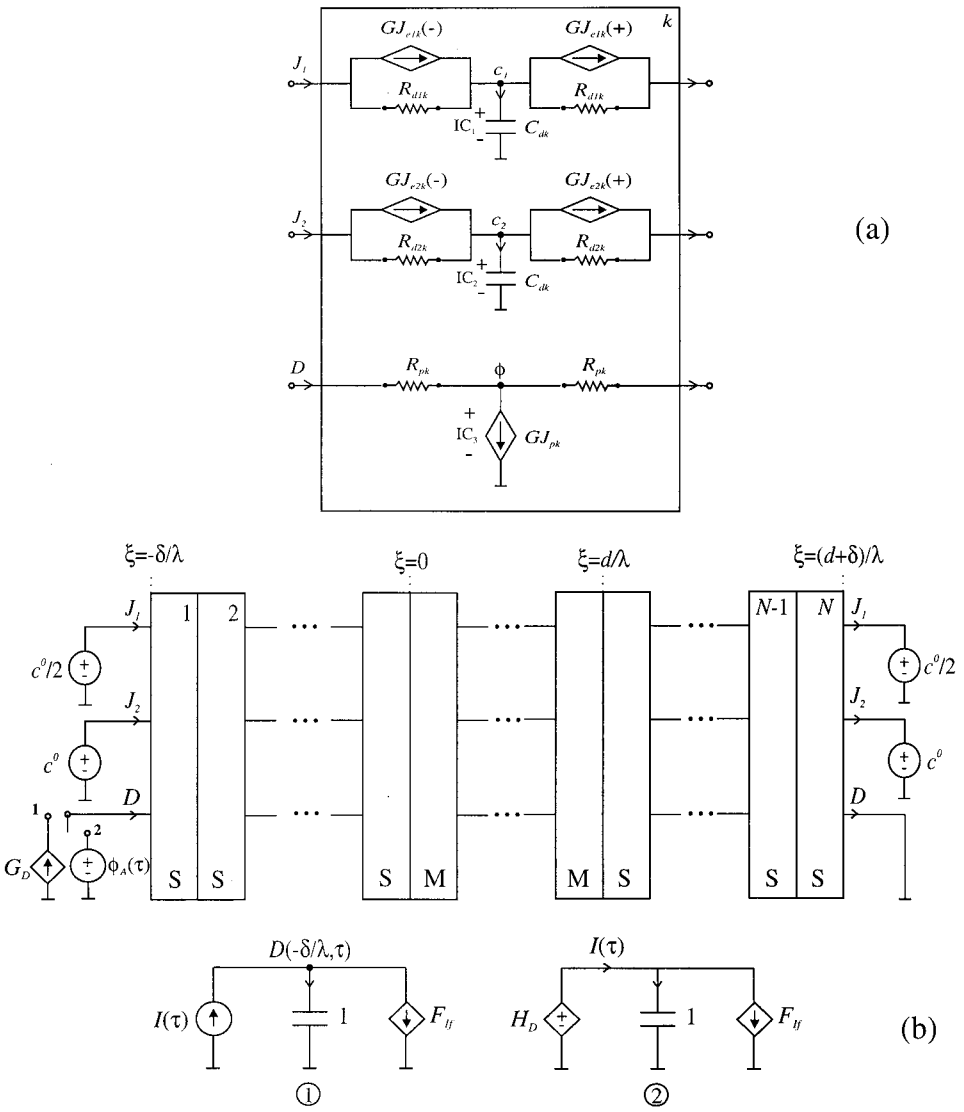

Figure 1. (a) Network model for the electrodiffusion in a volume element. (b) Network model for an ion-exchange membrane system. Details of the structures of boxes $1-N$ are shown in (a). Letters S and M indicate solution and membrane phases, respectively.

constant concentrations $c^0/2$ and c^0 there, $c^0 = c'^0/c_a$ being the dimensionless concentration of the bulk electrolyte solution. Equation 16a, which is obtained from eq 13, is a boundary condition for the time evolution of the electric displacement, **D**, at $\xi = -\delta/\lambda$,[26] and it is imposed when the electric current density, $I(\tau)$, is the externally controlled variable. When the electric potential, $\phi_A(\tau)$, is the externally applied perturbation, it is necessary to take into account the boundary condition given by eq 16b, instead of eq 16a; in this case, the electric current density through the system must be evaluated from eq 13. Finally, eq 17 defines the reference level for the electric potential.

2.2. Network Model. The network model representative of any transport process is obtained by dividing the physical region of interest, which we consider to have a unit cross-sectional area, into N volume elements or compartments of width δ_k ($k = 1, ..., N$), small enough for the spatial variations of the parameters within each compartment to be negligible.[27]

The network model for the electrodiffusion process in a compartment is shown in Figure 1a, and a complete explanation of it has been given elsewhere.[22] In this figure, the network elements are as follows: R_{dik} is the resistor representing the diffusion of ion i in the compartment k; $GJ_{eik}(\pm)$ is the voltage-controlled current source modeling the electrical contribution to the ionic flux, minus and plus signs meaning the flux entering and leaving the compartment k, respectively; C_{dk} is the capacitor representing the nonstationary effects of the electrodiffusion process in the compartment k; R_{pk} is the resistor modeling the constitutive equation of the medium; and GJ_{pk} is the voltage-controlled current source modeling the electric charge stores in the compartment k. The relation between those network elements and the parameters of the system is given by

$$R_{dik} = \frac{\delta_k}{2D_{ip}} \tag{18}$$

$$GJ_{eik}(\pm) = \pm D_{ip} z_i c_i\left(\xi_k \pm \frac{\delta_k}{2}\right)\frac{\phi(\xi_k) - \phi\left(\xi_k \pm \frac{\delta_k}{2}\right)}{\delta_k/2} \tag{19}$$

$$C_{dk} = \delta_k \tag{20}$$

$$R_{pk} = \frac{\delta_k}{2\epsilon} \tag{21}$$

$$GJ_{pk} = -\delta_k[z_1 c_1(\xi_k) + z_2 c_2(\xi_k) - \theta(\xi_k)] \tag{22}$$

For network modeling purposes, any number N of circuit elements such as those in Figure 1a must be connected in series

to form a network model for the entire physical region undergoing a diffusion−migration process.

Figure 1b shows the network model for the membrane system. In this figure, the details of the structures of boxes 1, ..., N are shown in Figure 1a, and the letters S and M indicate solution ($D_{ip} = D_{iS}$ and $\theta = 0$) and membrane ($D_{ip} = D_{iM}$ and $\theta = 1$) phases, respectively. In the network model of Figure 1b, the time-independent concentrations of the species of charges $z_1 = 2$ and $z_2 = -1$ in the membrane bathing solutions (eqs 14 and 15) are respectively represented by independent voltage sources of values $c^0/2$ and c^0. The origin of the electric potential (eq 17) is introduced into the network model by short-circuiting the node ϕ at $\xi = (d + \delta)/\lambda$. Subcircuit-1 is used to model the boundary condition given by eq 16a when switch-1 is on, and a complete explanation of it has been given elsewhere.[22,24] In this subcircuit F_{If}, given by

$$F_{If} = z_1 J_1\left(-\frac{\delta}{\lambda},\tau\right) + z_2 J_2\left(-\frac{\delta}{\lambda},\tau\right) \tag{23}$$

is the current-controlled current source modeling the faradaic electric current density; the independent current source models the external electric current density, $I(\tau)$; the current through the capacitor of unit capacitance is the displacement electric current density because the voltage through this capacitor is $\mathbf{D}(-\delta/\lambda,\tau)$; G_D, given by

$$G_D = \mathbf{D}\left(-\frac{\delta}{\lambda},\tau\right) \tag{24}$$

is a voltage-controlled current source which permits the value of $\boldsymbol{D}(-\delta/\lambda,\tau)$ obtained in subcircuit-1 to be imposed as a boundary condition to the Poisson equation. Finally, subcircuit-2 is used, when switch-2 is on, for computing the electric current density given by eq 13 in situations where the electric potential is the external perturbation. In this case, the electrical perturbation is represented by an independent voltage source of value $\phi_A(\tau)$; F_{If}, given by eq 23, models the faradaic electric current density again; and H_D, given by

$$H_D = \mathbf{D}\left(-\frac{\delta}{\lambda},\tau\right) \tag{25}$$

is a current-controlled voltage source which permits $\mathbf{D}(-\delta/\lambda,\tau)$ to be considered as a voltage-type variable. In this way, the current through the capacitor of unit capacitance is the displacement electric current density and the current through H_D is the total electric current density.[24]

3. Network Simulation

By means of the network model of Figure 1b, with the appropriate numerical values for the system parameters, the quantitative simulation of the electrical properties of ion-exchange membranes including diffuse double layer effects can be easily obtained using an electric circuit simulation program such as PSpice.

We will use some of the potential applications of the network simulation method applying them to the study of the steady-state electrical properties, the chronopotentiometric response, the chronoamperometric response, and the small-amplitude ac response of ion-exchange membrane systems with X ranging from 1 to 10, $z_1 = 2$, $z_2 = -1$, $d = 50\lambda$, $\delta = 100\lambda$, $D_{1S} = D_{2S} = 1$, $D_{1M} = D_{2M} = 0.1$, $c^0 = 0.5$, $\epsilon = 1$, $N = 480$, and the compartment thickness, δ_k, given by

$$\delta_k = 3,\ k = 1, ..., 30 \text{ and } 451, ..., 480$$

$$\delta_k = 0.6,\ k = 31, ..., 40;\ 201, ..., 210;\ 271, ..., 280, \text{ and } 441, ..., 450$$

$$\delta_k = 0.05,\ k = 41, ..., 200 \text{ and } 281, ..., 440$$

$$\delta_k = 1.5,\ k = 211, ..., 270$$

It is worth noting that the values chosen for the parameters of the system are completely arbitrary. The values of N and δ_k were chosen to ensure good accuracy and moderate CPU times (3 min in most cases), using a PC-Pentium/350. On the other hand, this spatial grid takes into account that the membrane|solution interfacial regions have a size of about 4λ in each phase. The remaining parameters are similar to those used by Manzanares et al.,[21] except for the charge number and the diffusion coefficient of the mobile ions.

3.1. Steady-State Electrical Properties. Figure 2 gives the total electric current density and the ionic fluxes through the membrane system at the steady state as a function of the applied electric potential, for different fixed charge concentrations, namely $X = 1$, 2, 5, and 10. Interestingly, as the applied electric potential is positive, the coions ($z_2 = -1$) move from the membrane to the solution at the left interface and from the solution to the membrane at the right interface. In this way, the left interface is reverse biased, while the right interface is forward biased.[19] Figure 2a shows the steady-state current−voltage characteristic for the whole membrane system. In this figure, an approximately ohmic behavior (underlimiting current regime) is observed followed by a region in which the electric current density varies very slowly with voltage (overlimiting current regime). In the lower voltage range, the slope of the current−voltage curves increases as the fixed charge concentration, X, increases. However, in the higher voltage region, this slope decreases as X increases. In this way, a limiting value for the total electric current density is expected in highly charged membrane systems. It is interesting to note that the classical expression for the limiting electric current density can be estimated theoretically as the current density that leads to zero concentration at the left membrane|solution interface when the electroneutrality condition is employed to describe transport in the diffusion boundary layer.[21] Thus, if we make use of the assumption of ideal permselectivity of the membrane system (i.e., zero coion flux), the limiting electric current density, I_L, can be written as

$$I_L = \frac{(z_1 - z_2)D_{1S}c^0\lambda}{\delta} \tag{26}$$

and for the systems here studied one obtains $I_L = 0.015$. Figure 2b shows the steady-state ionic fluxes−voltage characteristics for the whole membrane system. In this figure it is observed that the counterion flux, J_1, presents a similar behavior to that of the total electric current density, while the coion flux, J_2, decreases as the fixed charge concentration, X, increases, whatever the applied voltage may be, because in cation-exchange membranes the electric current density is carried mainly by the counterion.

On the other hand, Figures 3−5, respectively, exhibit the steady-state profiles of the ionic concentrations, the electric charge density, and the electric potential in the left (a) and in the right (b) ion-exchange membrane|solution interfaces, for a weakly charged membrane with $X = 1$ and various values of the applied electric current density in the underlimiting regime, namely $I = 0$, 0.005, 0.01, and 0.015.

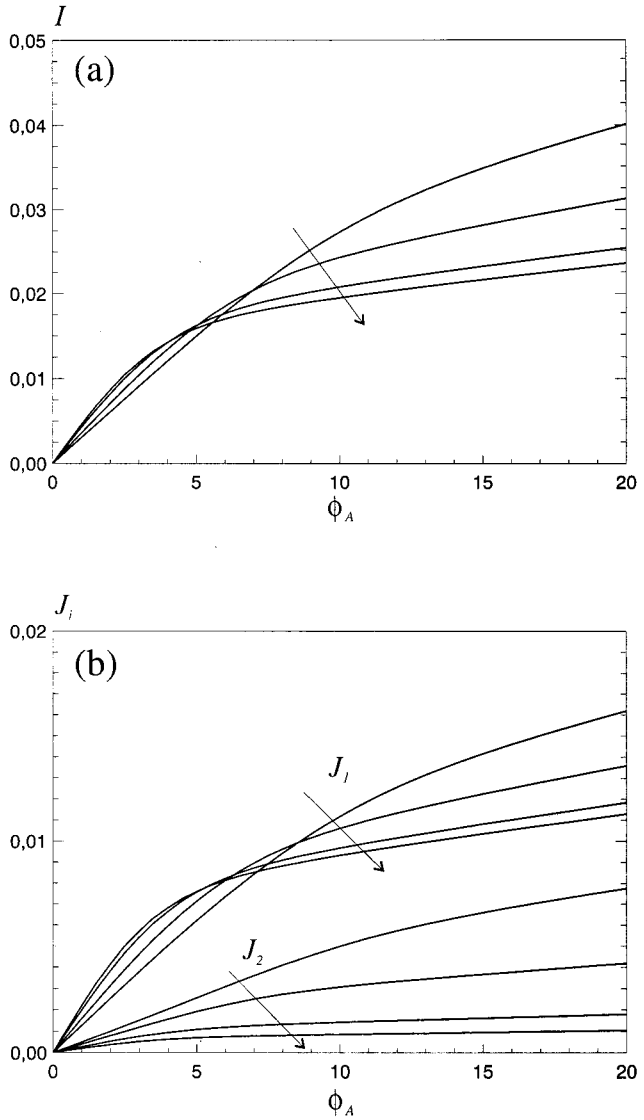

Figure 2. Steady-state current−voltage (a) and ion fluxes−voltage (b) characteristic of membrane systems with $z_1 = 2$, $z_2 = -1$, $d = 50\lambda$, $\delta = 100\lambda$, $D_{1S} = D_{2S} = 1$, $D_{1M} = D_{2M} = 0.1$, $c^0 = 0.5$, $\epsilon = 1$, and the fixed charge concentrations $X = 1$, 2, 5, and 10. The arrows indicate increasing values of X.

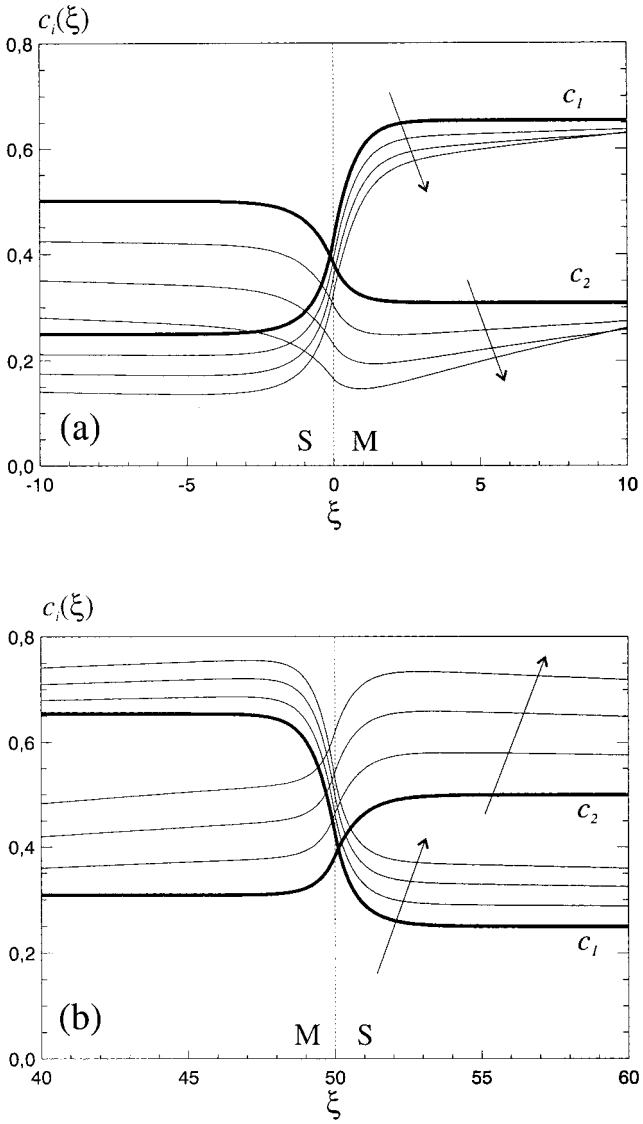

Figure 3. Detail of the concentration profiles at the left (a) and right (b) interfaces for a membrane system with $X = 1$, $z_1 = 2$, $z_2 = -1$, $d = 50\lambda$, $\delta = 100\lambda$, $D_{1S} = D_{2S} = 1$, $D_{1M} = D_{2M} = 0.1$, $c^0 = 0.5$, and $\epsilon = 1$, for the electric current densities $I = 0$, 0.005, 0.010, and 0.015. The arrows indicate increasing values of I.

In the equilibrium state of the system ($I = 0$), the electroneutral ionic concentrations and the electric potential profiles (see Figures 3 and 5) are uniform from $\xi = -100$ to $\xi \approx -4$ and from $\xi \approx 54$ to $\xi = 150$. From $\xi \approx -4$ to $\xi \approx 4$ and from $\xi \approx 46$ to $\xi \approx 54$, diffuse double-layer effects predominate and large deviations from local electroneutrality occur. It is worthy of note that the positive diffuse space charge in the regions $-4 < \xi < 0$ and $50 < \xi < 54$ is due entirely to mobile ions, and the negative membrane space charge in the regions $0 < \xi < 4$ and $46 < \xi < 50$ is due to both fixed and mobile ions. From $\xi \approx 4$ to $\xi \approx 46$, the profiles of the electroneutral ionic concentrations and the electric potential are again uniform and they obey the well-known Donnan equilibrium relations, which assume that the ionic concentrations and the electric potential are uniform up to (but discontinuous at) the ion-exchange membrane|solution interfaces. In this case, the analytical solution for the Donnan potential, ϕ_D, must be obtained by solving the following equation numerically:

$$e^{-2\phi_D} - e^{\phi_D} = \frac{X}{c^0} \tag{27}$$

Then, the uniform ionic concentrations in the membrane bulk, c_1* and c_2*, can be obtained using the Boltzmann relationships, i.e.,

$$c_1^* = \frac{c^0}{2} e^{-2\phi_D} \tag{28}$$

$$c_2^* = c^0 e^{\phi_D} \tag{29}$$

The results we obtained for ϕ_D, c_1*, and c_2*, which have been evaluated in the middle point of the membrane, $\xi = d/2\lambda$, are shown in Table 1, and they are in good agreement with those obtained from eqs 27−29.

When $I > 0$, the electroneutral ion concentration profiles increase (decrease) linearly with the position from $\xi = 4$ to $\xi = 46$ (from $\xi = -100$ to $\xi \approx -4$ and from $\xi \approx 54$ to $\xi = 150$) due to the positive applied electric current density, as can be observed in Figure 3. The polarization effects are then apparent in the bulk of the diffusion boundary layers, but the ion concentrations are higher at $\xi = -100$ than at $\xi = -4$ and higher at $\xi = 54$ than at $\xi = 150$. Thus, as previously pointed

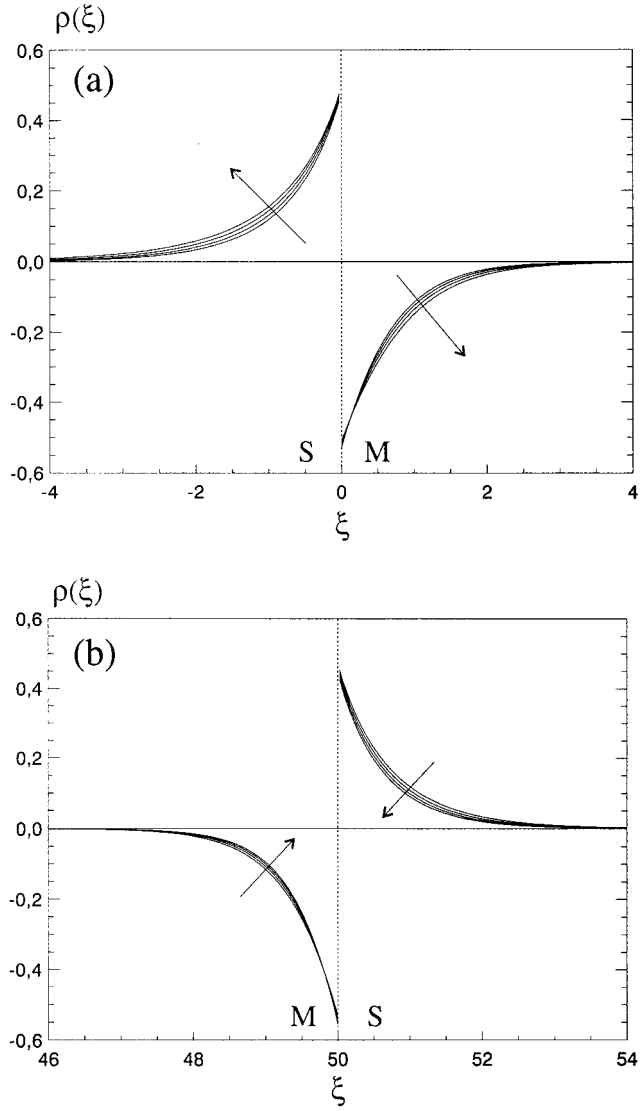

Figure 4. Detail of the electric charge density profiles at the left (a) and right (b) interfaces under the same conditions given in Figure 3.

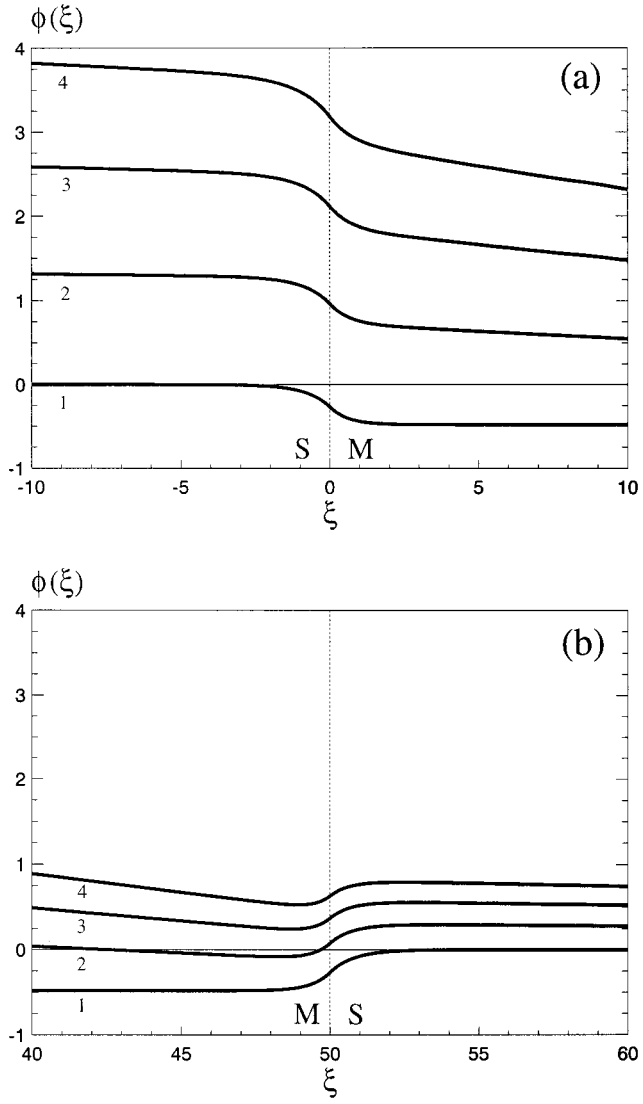

Figure 5. Detail of the electric potential profiles at the left (a) and right (b) membrane|solution interfaces for a membrane system with $X = 1$, $z_1 = 2$, $z_2 = -1$, $d = 50\lambda$, $\delta = 100\lambda$, $D_{1S} = D_{2S} = 1$, $D_{1M} = D_{2M} = 0.1$, $c^0 = 0.5$, and $\epsilon = 1$, for the following electric current densities: (1) $I = 0$; (2) $I = 0.005$; (3) $I = 0.010$; (4) $I = 0.015$.

out by Manzanares et al.,[21] the transfer of a positive electric current density through the membrane system causes a decrease in ion concentrations in the left diffusion boundary layer and an increase in the other. It can also be observed in Figure 3 that, due to the different charge numbers of the mobile ions, the variation of the coion concentration is higher than the variation of the counterion concentration, in contrast with the symmetric variation obtained by the authors above.

On the other hand, the electric charge density profiles (Figure 4) are typical for a negatively charged membrane and seem to be rather insensitive to an increase in the total electric current density, because the imposed electric current density generates electric fields that are smaller than those in the interfaces. In Figure 4, it can be seen that the thickness of the diffuse double layers in the reverse-biased interface, at $\xi = 0$, increase as I increases, while increase in the electric current density causes a decrease in the thickness of the diffuse double layers in the forward biased interface, at $\xi = 50$. These small changes in the electric charge density, ρ, with the applied electric current density, I, in Figure 4 result in dramatic changes in the electric potential, ϕ, as can be observed in Figure 5. As expected,[21] the electric potential varies almost linearly with position in the three bulk regions. The membrane system electric potentials obtained are $\phi(-\delta/\lambda) = 1.64$, 3.30, and 5.01 for $I = 0.005$, 0.01, and 0.015, respectively. The above results are in complete agreement with those of Manzanares et at.,[21] despite the different methods.

TABLE 1: Numerical Results Obtained for the Ionic Concentrations and the Electric Potential in the Middle Point of the Membrane, for a System with $z_1 = 2$, $z_2 = -1$, $d = 50\lambda$, $\delta = 100\lambda$, $D_{1S} = D_{2S} = 1$, $D_{1M} = D_{2M} = 0.1$, $c^0 = 0.5$, $\epsilon = 1$, and Various Values of the Fixed Charge Concentration

	ϕ_D	c_1*	c_2*
$X = 1$	−0.481	0.655	0.309
$X = 2$	−0.749	1.12	0.236
$X = 5$	−1.17	2.58	0.156
$X = 10$	−1.50	5.06	0.111

3.2. Chronopotentiometric Response. We now report the transient response of a membrane system to an externally applied electric current perturbation, $I(\tau)$. The initial conditions for the ionic concentrations and the electric potential correspond to the equilibrium values, and they are determined from a steady-state analysis for $I = 0$ as described in section 3.1. These initial conditions are included into the network model of Figure 1b via the initial voltages at the appropriate nodes of the network ("IC" in Figure 1a). The system is then perturbated with a step-

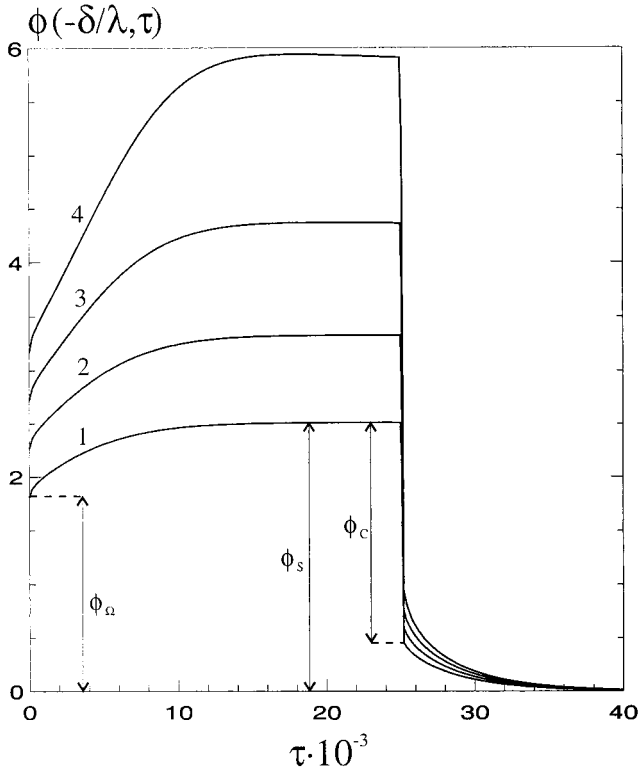

Figure 6. Time evolution of the electric potential drop across a membrane system with $X = 5$, $z_1 = 2$, $z_2 = -1$, $d = 50\lambda$, $\delta = 100\lambda$, $D_{1S} = D_{2S} = 1$, $D_{1M} = D_{2M} = 0.1$, $c^0 = 0.5$, and $\epsilon = 1$, in response to a pulse of electric current density of width $\tau_S = 25 \times 10^3$, for the following amplitudes: (1) $I_S = 0.01$; (2) $I_S = 0.0125$; (3) $I_S = 0.015$; (4) $I_S = 0.0175$.

function electric current density, given by

$$I(\tau) = \begin{cases} 0, & \tau = 0 \\ I_S, & 0 < \tau < \tau_S \\ 0, & \tau \geq \tau_S \end{cases} \tag{30}$$

where I_S is the amplitude of the electric current density and τ_S is the width of the square pulse.

The time evolution of the electric potential difference across a highly charged membrane system with $X = 5$, for $\tau_S = 25 \times 10^3$ and various values of the amplitude of the electric current density, namely $I_S = 0.01$, 0.0125, 0.015 and 0.0175, are shown in Figure 6. In this figure, it can be observed that, after an electric potential vertical jump, ϕ_Ω, due to the ohmic resistance of the system, the electric potential difference reaches a plateau after about 15×10^3 time units. Figure 6 shows that the ohmic potential jump, ϕ_Ω, increases as I_S increases. Moreover, this electric potential difference is directly proportional to the amplitude of the electric current density, I_S, because the resistance of the membrane system is constant. However, the plateau value of the electric potential difference across the membrane system, ϕ_S, is not directly proportional to I_S. In fact, this plateau value increases as I_S increases because in this system there is a limiting electric current density.[8] In this way, the total overvoltage, $\phi_S - \phi_\Omega$, increases as I_S increases. When the electric current density is switched off, after an electric potential vertical fall, ϕ_C, the potential difference across the membrane system reaches the zero value after about 15×10^3 time units. As shown in Figure 6, the concentration overvoltage, $\phi_S - \phi_C$, increases as I_S increases. These results are in good agreement with the experimental studies by Sistat and Pourcelly.[17]

3.3. Chronoamperometric Response. In this section, we report the transient response of the membrane system to an externally applied electric potential perturbation given by

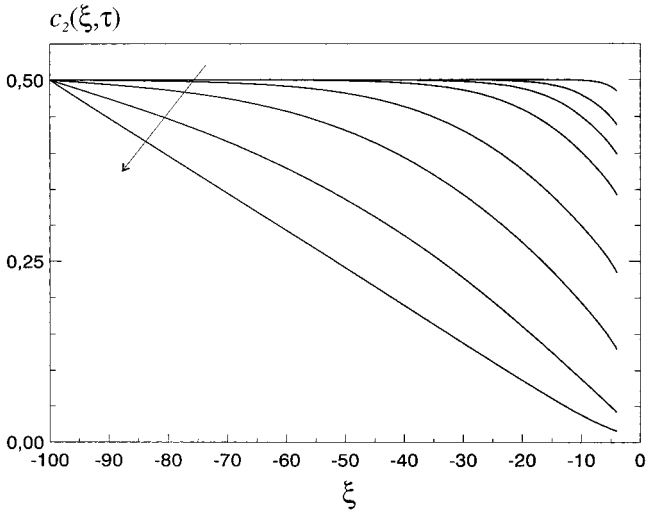

Figure 7. Time evolution of the coion concentration profile across the electroneutral region of the left diffusion boundary layer in a membrane system with $X = 5$, $z_1 = 2$, $z_2 = -1$, $d = 50\lambda$, $\delta = 100\lambda$, $D_{1S} = D_{2S} = 1$, $D_{1M} = D_{2M} = 0.1$, $c^0 = 0.5$, and $\epsilon = 1$, in response to a pulse of electric potential of amplitude $\phi_S = 8$, for the times $\tau = 10$, 50, 10^2, 2×10^2, 5×10^2, 10^3, 2×10^3, and 50×10^3. The arrows indicate increasing values of τ.

$$\phi_A(\tau) = \begin{cases} 0, & \tau = 0 \\ \phi_S, & \tau > 0 \end{cases} \tag{31}$$

where ϕ_S is the amplitude of the perturbating electric potential.

Figure 7 gives the time evolution of the coion concentration profile across the electroneutral region of the left diffusion boundary layer, when a highly charged membrane system with $X = 5$ is perturbated with a step-function electric potential of amplitude $\phi_S = 8$. In this figure it can be observed that the coion concentration near the membrane surface in the left diffusion boundary layer decreases gradually and the concentration profiles are only linear at times close to the steady state. In the nonstationary regime, the gradient of the ionic concentrations is not constant along all the section of the diffusion boundary layer. The switching on an electric potential leads to decrease of the ionic concentrations in the left diffusion boundary layer, first near the membrane surface, and during some time the ionic concentrations on the slightly larger distances are equal to the bulk ionic concentrations. These results show, on the basis of the Nernst−Planck and Poisson equations, that the concentration polarization of ion-exchange membranes increases in the time when the system is perturbated with a step-function electric potential, in accordance with the results obtained by other authors in ideal permselective membranes.[18]

On the other hand, the time evolution of the counterion flux exiting from the system, $J_1(d + \delta/\lambda,\tau)$, for a highly charged membrane system with $X = 5$ and various values of the amplitude of the perturbating electric potential, namely $\phi_S = 2$, 4, 6, 8, and 10, is shown in Figure 8. In this figure can be seen that the initial value of the counterion flux is higher than the steady-state value in the overlimiting regime, and the flux quickly decreases in time. These results show that during the transient period following the switching on a step-function electric potential, the ionic flux of the counterion removed from the membrane system is higher than in the steady-state. In this way, the use of transient techniques in ion-exchange membranes can lead to intensification of the efficiency of membrane processes such as electrodialysis.

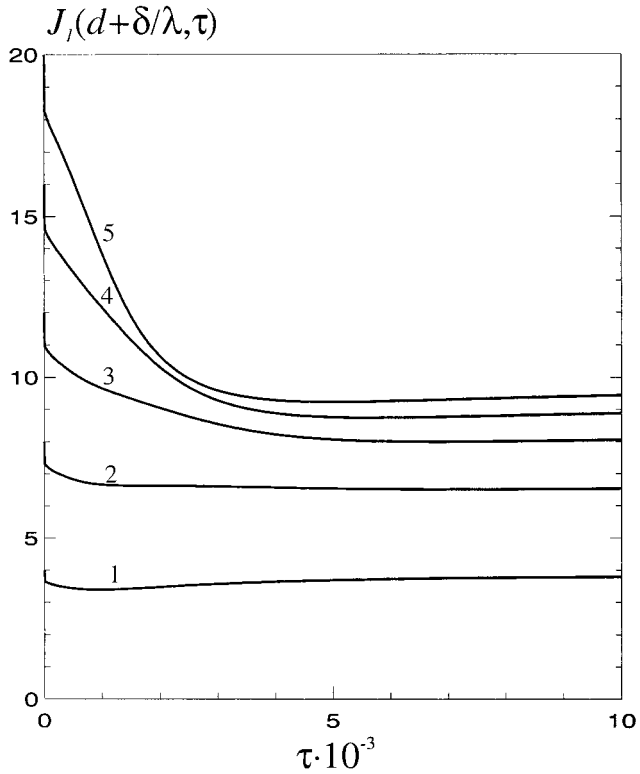

Figure 8. Time evolution of the counterion flux exiting from a membrane system with $X = 5$, $z_1 = 2$, $z_2 = -1$, $d = 50\lambda$, $\delta = 100\lambda$, $D_{1S} = D_{2S} = 1$, $D_{1M} = D_{2M} = 0.1$, $c^0 = 0.5$, and $\epsilon = 1$, in response to a pulse of electric potential of the following amplitudes: (1) $\phi_S = 2$; (2) $\phi_S = 4$; (3) $\phi_S = 6$; (4) $\phi_S = 8$; (5) $\phi_S = 10$.

3.4. Small-Amplitude ac Response. Finally, to illustrate another possibility offered by the network simulation method, we report the linear response of an ion-exchange membrane to a small-amplitude ac perturbation applied about the equilibrium state obtained in section 3.1. In this situation, the different variables describing the ionic transport in the system can be expressed as the sum of dc and ac components. In particular, the perturbing electric current density and the membrane system electric potential can be written as[28]

$$I(\tau) = I_{DC} + I_0 \sin(\omega\tau) \tag{32}$$

$$\phi\left(-\frac{\delta}{\lambda},\tau\right) = \phi_{DC} + \phi_0 \sin(\omega\tau + \theta) \tag{33}$$

where ω is the angular frequency, which is 2π times the conventional frequency f (in units of D_a/λ^2), I_0 and ϕ_0 ($\phi_0 \ll RT/F$) are the ac amplitudes of the perturbating electric current density and the electric potential difference, respectively, and θ is the phase difference between the voltage and the current. Now, the dimensionless electrochemical impedance Z (in units of $\lambda RT/F^2D_ac_a$) is a complex quantity given by the following equation:

$$Z(j\omega) = \frac{\phi_0}{I_0}e^{j\theta} = Z'(\omega) + jZ''(\omega) \tag{34}$$

where $j = (-1)^{1/2}$ is the imaginary number, and Z' and Z'' are the real and imaginary parts of the impedance, respectively.

In this paper, the real and imaginary parts of $Z(j\omega)$ are obtained by simulation of the network model shown in Figure 1b under ac conditions, and they are conveniently displayed in the form of a complex-plane impedance plot in which $-Z''(\omega)$ is plotted against $Z'(\omega)$ with the angular frequency ω as a parameter increasing from the right to the left of the plot.

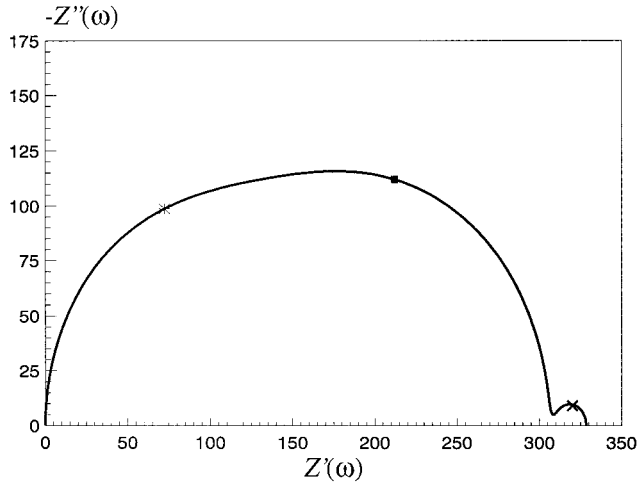

Figure 9. Complex-plane impedance plot for an ion-exchange membrane system with $X = 1$, $z_1 = 2$, $z_2 = -1$, $d = 50\lambda$, $\delta = 100\lambda$, $D_{1S} = D_{2S} = 1$, $D_{1M} = D_{2M} = 0.1$, $c^0 = 0.5$, $\epsilon = 1$, and $I_{DC} = 0$ ($\phi_{DC} = 0$). Marked points are (*) for $f_{1S} = 0.239$, (■) for $f_{1M} = 0.0466$, and (×) for $f_2 = 4.6 \times 10^{-5}$.

Figure 9 gives the complex-plane impedance plot of a weakly charged membrane system with $X = 1$, for $I_{DC} = 0$ ($\phi_{DC} = 0$). This impedance plot shows two regions: a geometric arc at high frequencies and a diffusional arc at low frequencies. In this figure it can be seen that the geometric arc is distorted and it can be considered as the combination of two different geometric arcs associated with the migration processes taking place in the bathing electrolyte solutions and in the membrane. In a first approximation, each geometric arc can be interpreted as the charging of the geometric capacitance, C_g, in parallel with the ohmic resistance, R_{ac}. The radius of each geometric semicircle is $R_{ac}/2$ and the peak frequency $f_1 = (2\pi R_{ac}C_g)^{-1}$. In this case, the geometric capacitances of the solution and membrane phases, C_{gS} and C_{gM} (in units of $F^2c_a\lambda/RT$), are given by[28]

$$C_{gS} = \frac{\epsilon\lambda}{2\delta} \tag{35}$$

$$C_{gM} = \frac{\epsilon\lambda}{d} \tag{36}$$

and the ohmic resistances, R_{acS} and R_{acM} (in units of $\lambda RT/F^2D_ac_a$), can be expressed as[29]

$$R_{acS} = \int_{-\delta/\lambda}^{0} \frac{d\xi}{\sum_{i=1}^{2} z_i^2 D_{iS} c_{iDC}(\xi)} + \int_{d/\lambda}^{(d+\delta)/\lambda} \frac{d\xi}{\sum_{i=1}^{2} z_i^2 D_{iS} c_{iDC}(\xi)} \tag{37}$$

$$R_{acM} = \int_{0}^{d/\lambda} \frac{d\xi}{\sum_{i=1}^{2} z_i^2 D_{iM} c_{iDC}(\xi)} \tag{38}$$

The solution of eqs 37 and 38 presents a serious problem because of the presence of space charge regions at the membrane|solution interfaces. However, if we use the assumption of local electroneutrality in the system and the Donnan equilibrium relations at the interfaces, we obtain the following equations:

$$R_{acS} = \frac{2\delta/\lambda}{z_1^2 D_{1S} c^0/2 + z_2^2 D_{2S} c^0} \quad (39)$$

$$R_{acM} = \frac{d/\lambda}{z_1^2 D_{1M} c_1^* + z_2^2 D_{2M} c_2^*} \quad (40)$$

On the other hand, the diffusional relaxation time of the membrane system is $\tau_D = d^2/D_{1M} = 2.5 \times 10^4$. Now, from eqs 35, 36, 39, and 40, one readily obtains $C_{gS} = 5 \times 10^{-3}$, $C_{gM} = 0.02$, $R_{acS} = 133.3$, and $R_{acM} = 170.7$. In this way, the peak frequencies of the solution and membrane geometric arcs are $f_{1S} = 0.239$ and $f_{1M} = 0.0466$, respectively, while the peak frequency of the diffusional arc is of the order of $\tau_D^{-1} = 4 \times 10^{-5}$. We have found here that the real part of the impedance at the intersection point between the geometric and diffusional arcs is $Z' = 308.4$, while the peak frequency of the diffusional arc is $f_2 = 4.6 \times 10^{-5}$. These results are then in good agreement with the theoretical expectations.

4. Conclusions

The network simulation method has been used to study the electrical properties of ion-exchange membranes including diffuse double-layer effects. A network model has been proposed for the Nernst−Planck and Poisson equations describing the ionic transport processes through a multilayer system composed by an ion-exchange membrane and two diffusion boundary layers on both sides of the membrane. We have shown that this model, together with an electric circuit simulation program, allows us to easily study the steady-state, transient, and small-amplitude ac responses of ion-exchange membranes, whatever the experimental conditions may be.

Although we are aware that excellent work has already been carried out in this field, we believe that the results here presented can contribute to a better understanding of the ionic transport through ion-exchange membranes. Therefore, we have analyzed both the steady-state current−voltage characteristic and the structure of the equilibrium and nonequilibrium diffuse double layers in cation-exchange membranes with an asymmetric electrolyte solution and unequal ionic diffusivities in the membrane and the solution phases, and the transient responses of a nonideal membrane system to impulses of electric current density and electric potential. We have found that, during the transient period following the switching on a step-function electric potential in the overlimiting regime, the ionic flux of the counterion removed from a highly charged membrane system is higher than in the steady state. In this way, the use of transient techniques in ion-exchange membranes can lead to intensification of the efficiency of membrane processes such as electrodialysis. An original study of the small-amplitude ac response of the whole membrane system (membrane, diffuse double layers, and diffusion boundary layers) is also reported.

Acknowledgment. The authors acknowledge the financial support received from the DGES, Ministry of Education and Culture of Spain, through Project PB96-0425.

References and Notes

(1) Helfferich, F. *Ion Exchange*; McGraw-Hill: New York, 1962.
(2) Lakshminarayanaiah, N. *Transport Phenomena in Membranes*; Academic Press: New York, 1969.
(3) Rubinstein, I. *Electro-Diffusion of Ions*; SIAM Studies in Applied Mathematics: Philadelphia, 1990.
(4) Mafé, S.; Aguilella, V. M.; Pellicer, J. *J. Membr. Sci.* **1988**, *36*, 497.
(5) Guirao, A.; Mafé, S.; Manzanares, J. A.; Ibañez, J. A. *J. Phys. Chem.* **1995**, *99*, 3387.
(6) Castilla, J.; García-Hernández, M. T.; Hayas, A.; Horno, J. *J. Membr. Sci.* **1996**, *116*, 107.
(7) Castilla, J.; García-Hernández, M. T.; Moya, A. A.; Hayas, A.; Horno, J. *J. Membr. Sci.* **1997**, *130*, 183.
(8) Rubinstein, I.; Shtilman, L. *J. Chem. Soc., Faraday Trans. 2* **1979**, *75*, 231.
(9) Hainsworth, A. H.; Hladky, S. B. *Biophys. J.* **1987**, *51*, 27.
(10) Nikonenko, V. V.; Zabolotskii, V. I.; Gnusin, N. P. *Sov. Electrochem.* **1989**, *25*, 262.
(11) Listovnichii, A. V. *Sov. Electrochem.* **1991**, *27*, 284.
(12) Gurevich, Yu. Ya.; Noskov, A. V.; Kharkats, Yu. I. *Sov. Electrochem.* **1991**, *27*, 605.
(13) Manzanares, J. A.; Kontturi, K.; Mafé, S.; Aguilella, V. M.; Pellicer, J. *Acta Chem. Scand.* **1991**, *45*, 115.
(14) Tanaka, Y. *J. Membr. Sci.* **1991**, *57*, 217.
(15) Taky, M.; Pourcelly, G.; Lebon, F.; Gavach, C. *J. Electroanal. Chem.* **1992**, *336*, 171.
(16) Chapotot, A.; Pourcelly, G.; Gavach, C.; Lebon, F. *J. Electroanal. Chem.* **1995**, *386*, 25.
(17) Sistat, P.; Pourcelly, G. *J. Membr. Sci.* **1997**, *123*, 121.
(18) Mishchuk, N. A.; Koopal, L. K.; González-Caballero, F. *Proc. IAP-97*; Wageningen: The Netherlands, 1997; pp 1−18.
(19) Bassignana, I. C.; Reiss, H. *J. Phys. Chem.* **1983**, *87*, 136.
(20) Selvey, C.; Reiss, H. *J. Membr. Sci.* **1987**, *30*, 75.
(21) Manzanares, J. A.; Murphy, W. D.; Mafé, S.; Reiss, H. *J. Phys. Chem.* **1993**, *97*, 8524.
(22) Moya, A. A.; Castilla, J.; Horno, J. *J. Phys. Chem.* **1995**, *99*, 1292.
(23) Horno, J.; Moya, A. A.; González-Caballero, F. *J. Phys. Chem.* **1995**, *99*, 12283.
(24) Horno, J.; Moya, A. A.; González-Fernández, C. F. *J. Electroanal. Chem.* **1996**, *402*, 73.
(25) Buck, R. P. *J. Membr. Sci.* **1984**, *17*, 1.
(26) Murphy, W. D.; Manzanares, J. A.; Mafé, S.; Reiss, H. *J. Phys. Chem.* **1992**, *96*, 9983.
(27) Speiser, B. In *Electroanalytical Chemistry*; Bard, A. J., Rubistein, I., Eds.; Marcel Dekker: New York, 1996; Vol. 19, p 64.
(28) Macdonald, J. R., Ed. *Impedance Spectroscopy*; Wiley: New York, 1987.
(29) Brumleve, T. R.; Buck, R. P. *J. Electroanal. Chem.* **1978**, *90*, 1.